Desalination and Water Treatment
www.deswater.com

doi: 10.5004/dwt.2021.27012

220 (2021) 246–254
April

Combination of zero-valent iron and persulfate radical under ultraviolet irradiation for enhanced phenol degradation

Mahdi Salehzadeh[a], Arezoo Nejaei[a,*], Mohammad Ebrahim Ramazani[a], Mohammad Shokri[b], Parvin Alizadeh Eslami[b]

[a]*Department of Environment, Tabriz Branch, Islamic Azad University, Tabriz, Iran, emails: arezoonejaei@yahoo.com (A. Nejaei), rojinajansr@gmail.com (M. Salehzadeh), ramazani_m_a@yahoo.com (M.E. Ramazani)*
[b]*Department of Chemistry, Tabriz Branch, Islamic Azad University, Tabriz, Iran, emails: shokri@iaut.ac (M. Shokri), sp.alizadeh@gmail.com (P. Alizadeh Eslami)*

Received 21 May 2020; Accepted 30 December 2020

ABSTRACT

Phenolic compounds, a group of typical hazardous synthetic organic pollutants, are one of the most common contaminants in industrial wastewater. The efficiency of the advanced oxidation process, which is the combination of zero-valent iron (ZVI) and persulfate radical under ultraviolet irradiation was studied for enhanced phenol degradation. Experiments were conducted in a 3 L plexiglass reactor equipped with two UV irradiation sources (254 nm). The effect of variables such as initial pH, ZVI dose, persulfate (PS) dose, phenol concentration, and contact time were investigated. Co-existing effect of cations including Na^+, K^+, Ca^{2+}, Mg^{2+}, and Al^{3+} and anions including F^-, Cl^-, HCO_3^-, NO_3^-, SO_4^{2-}, CO_3^{2-}, and PO_4^{3-} on degradation efficiency of phenol was investigated using ZVI/PS/UV process. The results showed that the highest phenol removal was obtained at initial pH 5. The optimal dose of ZVI was 0.8 mmol/L and 94.87% ± 3.85% phenol removal was obtained at pH 5 and a reaction time of 30 min. Increasing the PS dose to higher than 0.5 mmol/L did not show any positive effect on phenol removal because of $SO_4^{-\bullet}$ consumption. Inhibiting and promoting the effect of some co-existing anions on phenol degradation efficiency was observed in the order of $HCO_3^- > Cl^- > PO_4^{3-} > F$ and $CO_3^{2-} > NO_3^- > SO_4^{2-}$, respectively. However, the co-existence of cations has a significant effect on the phenol degradation efficiency by ZVI/PS/UV process in the order of $Al^{3+} > Ca^{2+} > Mg^{2+} > K^+ > Na^+$. The addition of glucose as a quencher in the initial solution showed that the $^\bullet OH$ and $SO_4^{-\bullet}$ radicals were the main radical species in the ZVI/PS/UV process for phenol removal.

Keywords: Persulfate radical; Phenolic compounds; Ultraviolet irradiation; Zero-valent iron

1. Introduction

One of the most important concerns for environmental protection is industrial wastewater that may contain various pollutants such as hazardous organic and inorganic compounds from textile, cosmetic, pharmaceutical industries, agriculture, and urban activities [1–3].

Phenolic compounds are a group of typical hazardous synthetic organic pollutants with low biodegradability compared to the nitro-substituted and chlorinated phenolic compounds [4,5]. They are one of the most common pollutants in industrial wastewater, coming from paper mills, textile, paints, and petrochemical industries posing threats to public health, environment, and aquatic ecosystems [6,7].

* Corresponding author.

The reaction between phenol with chlorine and nitro groups may cause chlorophenol and nitrophenol formation. Moreover, it is well-established that phenol and its derivatives have adverse health effects on humans, even at very low concentrations. Some have claimed that phenol causes health effects such as impairment of the pancreas, liver, kidney and they may be the cause for paralysis of the central nervous system [8,9]. Therefore, phenol-containing water or wastewater must be treated before being discharged into the environment.

There are various methods to remove phenol from water and wastewater such as physical, chemical, and biological methods [6,10–11]. Some reported that membrane biological reactors (MBR) efficiently remove phenol (>98.5%) from industrial hypersaline wastewater [12]. Although in another study, a combination of ultrafiltration hollow fiber membrane with photo-ferrioxalate and Fenton's reaction was used for the efficient treatment of phenol [13]. Membrane-based separation is another method applied to industrial wastewater treatment. These methods have advantages such as the least installation complexity, needing low space, low energy consumption, as well as high removal efficiency. However, certain problems like fouling by particulate matter restrict their application [6,14].

Adsorption is another effective method used for the removal of organic pollutants from water or wastewater by various adsorbents. Low cost and high removal efficiency are the important reasons for turning to such methods [15,16]. Zero-valent iron (ZVI) nanoparticle is another matter introduced for phenol removal by other researchers.

The advanced oxidation processes (AOPs) are important methods frequently and effectively used for industrial wastewater treatment. These methods can produce hydroxyl radicals (OH) or sulfate radicals ($SO_4^{-\bullet}$) considered as a strong oxidant able to oxidize and remove refractory organic matters, traceable organic contaminants, or certain inorganic pollutants [17]. In these processes, ozone (O_3), UV, hydrogen peroxide (H_2O_2), and persulfate compounds can be used [18].

Removal of phenol have been reported by catalytic oxidative using iron oxide promoted sulfonate d-ZrO_2 by AOPs and results have shown that total phenol mineralization occurred within 15 min was 88% in 6 h [19]. Another study addressing phenol removal is the photoelectrochemical under solar light with polyaniline-modified TiO_2 electrodes. This study claimed that the presence of polyaniline increases the conductivity of the electrode [20].

Based on studies, photoelectrocatalytic methods have the advantages like the possibility to remove toxic and persistent organic compounds, even at low concentrations [21]. Recently, the generation of sulfate radical ($SO_4^{-\bullet}$)-based AOPs has attracted attention to treat various wastewater because it has been proven that the amount of redox potential of sulfate radical (2.5–3.1 V) is greater than hydroxyl radical (1.9–2.7 V) [22,23].

The source of $SO_4^{-\bullet}$ is often from peroxydisulfate ($S_2O_8^{2-}$), a strong and stable oxidizing agent [24]. This active radical can be generated through different methods including transition metals (Me^{n+}), ultraviolet light, thermal energy, microwave, ultrasound, and strong basic solutions by reactive with persulfate anions [25,26].

Among various transition metal catalysts, Fe is relatively nontoxic and inexpensive; so, it has been used to activate persulfate oxidation. Various types of Fe-based catalysts can be used for the chemical activation of persulfate, like nano-sized ZVI (Fe^0) [27] and ZVI powder [28]:

$$S_2O_8^{2-} + Me^{n+} \longrightarrow SO_4^{-\bullet} + Me^{(n+1)+} + SO_4^{2-} \quad (1)$$

The generation of $SO_4^{-\bullet}$, the activating agent including UV radiation, thermal energy, microwave, ultrasonic radiation (US), and strong basic solution were used as Eqs. (2)–(5):

$$S_2O_8^{2-} + h\nu \longrightarrow 2SO_4^{-\bullet} \quad (2)$$

$$S_2O_8^{2-} \xrightarrow{heat} SO_4^{-\bullet} \quad (3)$$

$$S_2O_8^{2-} \xrightarrow{US} SO_4^{-\bullet} \quad (4)$$

$$2S_2O_8^{2-} + 2H_2O \xrightarrow{OH^-} 3SO_4^{2-} + SO_4^{-\bullet} + O_2^{-\bullet} + 4H^+ \quad (5)$$

It was reported that the fast reaction rate constant between ferrous ions and $SO_4^{-\bullet}$ leads to the $SO_4^{-\bullet}$ consumption by excess ferrous ions [29]. Thus, to solve such a problem, ZVI has been used as an alternative of dissolved iron ions since it slowly releases iron ions [30,31]. Next studies showed that the combined process of ZVI and sulfite (ZVI/sulfite) reveals good degradation efficiencies for organic pollutants [32].

Some reported that the dominant activator of sulfite in this process (ZVI/sulfite) is a slow release of iron ions, i.e. the decomposition of ferric sulfite complex should be a rate-determining step [31]. Other researchers proposed photo-irradiation to improve the degradation efficiency of organic pollutants in ZVI/sulfite process. They used it for propranolol (PrP) removal and achieved good results for the removal of this pollutant [33]. Recently, few studies have been reported on the application of the ZVI/PS/UV process in the removal of organic matter. Based on this idea, we decided to use this process for the removal of phenol from synthetic wastewater. This study was aimed at investigating variables like phenol concentration, solution pH, contact time, persulfate concentration, and effect of organic matter, anions and cations, and ZVI dose on phenol removal efficiency.

2. Materials and methods

2.1. Chemicals

ZVI was supplied by Sigma-Aldrich and phenol (C_6H_5OH) was purchased from Merck Co. (Darmstadt, Germany). Diluted NaOH and HCl (1 M) were used to adjust the pH of the solutions. All solutions were prepared with deionized water. The stock solution of sodium persulfate at a concentration of 1 mol/L was freshly prepared using deionized water. All of the stock solutions prepared here were stored at 4°C in a refrigerator.

2.2. Experimental procedures

All experiments were conducted in a 3 L plexiglass reactor equipped with a thermostat and stirrer (50 rpm) (Fig. 1).

Two UV lamps were used as UV irradiation sources (254 nm, Philips Co. , Netherlands). The desired concentrations of ZVI, PS, and phenol were continuously fed and mixed in the reactor. The samples withdrawn at predetermined time intervals were filtered through a paper filter (Whatman no. 41) and measured immediately. All tests were conducted at duplicate, and the error bars shown in all data plots represent the standard deviation among the replicate test results.

2.3. Sample analysis

The concentration of phenol was measured by a colorimetric method [34]. To 100 mL of samples, 2.5 mL of NH_4OH solution was added, immediately adjusted to pH 7.9 ± 0.1 with phosphate buffer. Then, 1 mL of 4-aminoantipyrine and $K_3Fe(CN)_6$ solution was added and mixed well. After 15 min, the samples were placed in a spectrophotometer cuvette and absorbance was measured at 500 nm against a blank. Absorbance values were converted to phenol concentrations in the sample by using the calibration curve.

3. Results and discussion

3.1. Phenol degradation under different process combination

To determine synergetic effects, the ZVI/UV, PS/UV, and combination of ZVI/PS/UV process were conducted for phenol degradation from synthetic wastewater. Fig. 2 shows the results of phenol degradation efficiency with different process combinations.

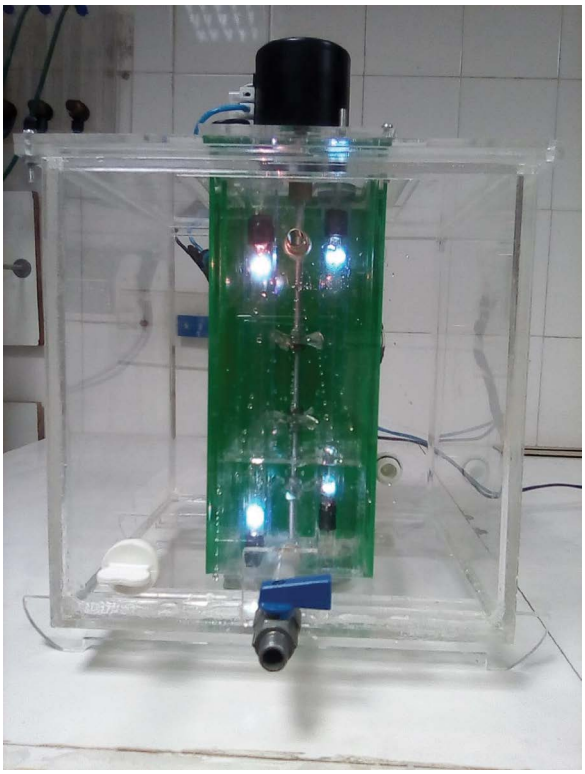

Fig. 1. Photograph of photoreactor.

As seen in Fig. 2, the combination of ZVI and PS radicals under UV irradiation significantly enhanced the phenol degradation efficiency at a solution pH of 6. The phenol degradation efficiency was negligible ZVI/UV process and reached to 8.05% removal efficiency after 60 min reaction time. However, the phenol degradation efficiency underwent relatively high degradation under PS/UV process (49.48% after 60 min), while phenol degradation efficiency with a combination of ZVI/PS/UV process occurred at the highest degradation efficiency (94.74% after 60 min reaction time). The phenol degradation rates measured under different process combination could conveniently be compared in terms of first order rate constants, obtained from the slopes of plots of Fig. 3.

The initial rate of phenol degradation of 15 mg/L with a combination of ZVI/PS/UV process (0.051 mg/L min) was five times higher than PS/UV process (0.011 mg/L min) and five times higher than ZVI/UV process (0.001 mg/L min). Synergetic effect of ZVI/UV, PS/UV, and combination of ZVI/PS/UV process was calculated by Eq. (6):

$$\text{Synergetic Effect} = \frac{k_{\text{ZVI/PS/UV}}}{k_{\text{PS/UV}} + k_{\text{ZVI/UV}}} \tag{6}$$

As Eq. (6) demonstrated, the synergistic effect between ZVI/UV and PS/UV process might be quantified as the normalized difference between the rate constants obtained under the combination of ZVI/PS/UV process and the sum of the separate ZVI/UV and PS/UV process rate constants. The rate constant of the ZVI/PS/UV process combination was fourfold (0.051/0.012) that of the sum of the individual processes.

3.2. Effect of solution pH on ZVI/PS/UV process efficiency

To determine the optimal solution pH of the ZVI/PS/UV process, the experiments were conducted at various initial pH values (about 2–8) with an initial phenol concentration of 15 mg/L as illustrated in Fig. 4.

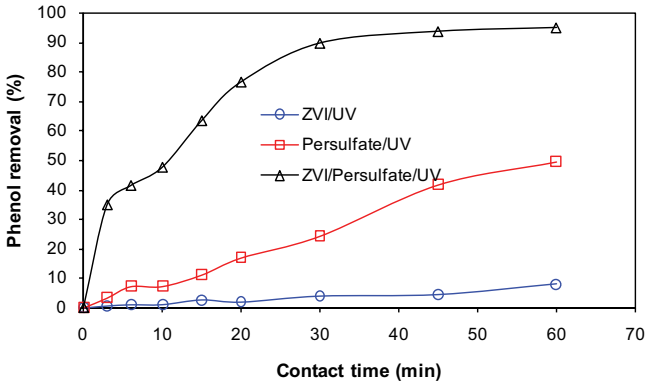

Fig. 2. Phenol removal with different process combination (initial phenol concentration: 15 mg/L, ZVI dose: 0.1 mmol/L, PS dose: 0.2 mmol/L, solution pH: 6, and reaction time: 30 min).

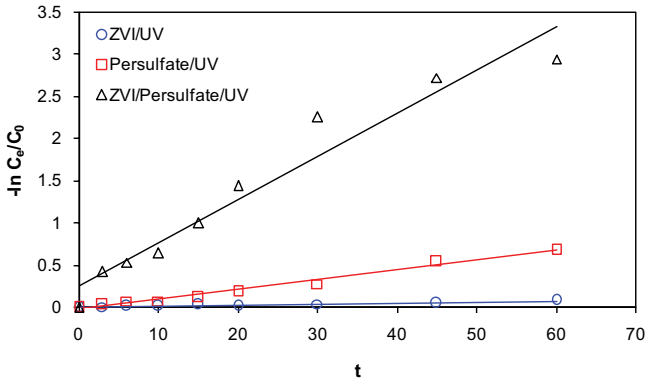

Fig. 3. First-order kinetic plots of phenol degradation with different process combination.

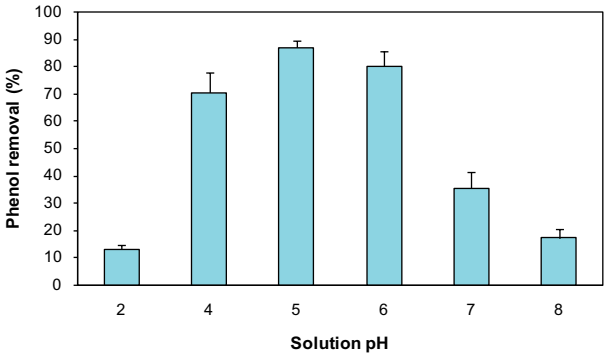

Fig. 4. Effect of solution pH on phenol degradation efficiency (initial phenol concentration: 15 mg/L, ZVI dose: 0.1 mmol/L, PS dose: 0.2 mmol/L, and reaction time: 30 min).

Fig. 4 shows that with increasing solution pH from 2 to 5, the phenol degradation efficiency increased from 13.02% ± 1.67% to 86.89% ± 2.51%. The steepness trend of phenol degradation efficiency was observed with increasing solution pH higher than 5. With increasing solution pH from 5 to 8, the phenol degradation efficiency declined from 86.89% ± 2.51% to 17.26% ± 3.05%.

According to the morphological distribution curves of S(IV), Fe^{2+}, and Fe^{3+}, pH can directly influence the form of iron ions and S(IV) in the reaction solution, as a result of affecting the degradation of organic pollutants when using iron-activated sulfate system [35]. At near-neutral or week acidic circumstances (solution pH: 4–6), similar oxidation efficiencies were achieved, like a previous study using an iron/sulfate system to treat wastewater [36]. It is suggested that HSO_3^- containing the highest ability to complex Fe^{2+} and Fe^{3+} was the dominant species of S(IV) in the pH range of 4–6 [37], which could explain the high removal efficiency of phenol in the pH range of 4–6. Thus, the degradation efficiencies of phenol were nearly stable when the initial pH values were 4.0, 5.0, and 6.0. Although Fe^{2+} and Fe^{3+} could be produced by hydrogen evolution corrosion, plenty of S(IV) exists in the species of SO_2 (aq) at pH 2 and 3, decreasing the concentration of HSO_3^- as a result of reducing the phenol removal efficiency [37]. The significantly decreased removal efficiency of phenol at solution pH higher than 6 would be due to the lower HSO_3^- species, hydrolysis of iron ions, as well as the formed passive film on the surface of ZVI [31].

3.3. Effect of ZVI dose on ZVI/PS/UV process efficiency

Under an optimal solution pH of 5, the effect of ZVI dose on the degradation efficiency of the ZVI/PS/UV process was investigated in suspensions containing 15 mg/L of phenol, and it was 0.2 mmol/L of PS radicals. The degradation efficiency of phenol was measured under different reaction times shown in Fig. 5.

Results in Fig. 5 revealed that with increasing ZVI does from 0.1 to 0.8 mmol/L, the phenol degradation efficiency increased from 22.7% ± 6.93% to 94.87% ± 3.85%. This might have been attributed to increased active sites with increasing ZVI dose, enhancing the decomposition of $S_2O_8^{2-}$ and led to a high phenol removal efficiency [38]. However, further increasing the ZVI dose above 0.8 mmol/L did not bring about further improvement in the phenol degradation efficiency. When 1 mmol/L of ZVI dose was used, the phenol degradation efficiency depleted and reached 91.38% ± 3.24%. This could have been ascribed to the excess Fe^{2+} produced by ZVI reacted with $SO_4^{-\bullet}$ as a radical scavenger according to Eq. (7) [39]:

$$Fe^{2+} + SO_8^{2-} \longrightarrow Fe^{3+} + SO_4^{2-} \quad (7)$$

3.4. Effect of concentration of PS radicals

The batch experiments under the combination of ZVI/PS/UV process with constant ZVI does (0.8 mmol/L) were conducted to investigate the effect of the initial concentration of PS radicals in the range of 0.1–0.6 mmol/L. Fig. 6 depicted variation of phenol degradation efficiency as a function of PS dose.

As observed in Fig. 6, the phenol degradation efficiency increased when the PS dose changed from 0.1 to 0.5 mmol/L (optimal PS dose). At this time, the phenol degradation efficiency enhanced from 62.79% ± 2.71% to 98.76% ± 0.33%. The higher efficiency can be attributed to the increased generation of $SO_4^{-\bullet}$ in the reactor, thus promoting interaction with the reactants.

Upon activation of $S_2O_8^{2-}$ ions, the radicals of $SO_4^{-\bullet}$, which are strong oxidants (E_0: 2.6 V), are produced within the system. These radicals can subsequently react with water molecules and produce highly active •OH radicals (E_0: 2.8 V). Together with •OH radicals, $SO_4^{-\bullet}$ radicals were capable of effectively breaking down the aromatic rings of phenol molecules [40]. However, a further increase in the initial PS concentration did not give rise to remarkable degradation performance since $SO_4^{-\bullet}$ consumed (Eq. (8)) [36]. Moreover, $SO_4^{-\bullet}$ $SO_4^{-\bullet}$ can combine with ZVI.

$$SO_4^{-\bullet} + SO_4^{-\bullet} \rightarrow 2SO_4^{2-} \quad k = 4.8 - 8.1 \times 10^8 M^{-1}S^{-1} \quad (8)$$

In other words, this behavior is because at amplified $SO_4^{-\bullet}$ concentrations, $S_2O_8^{2-}$ are produced, in turn utilizing

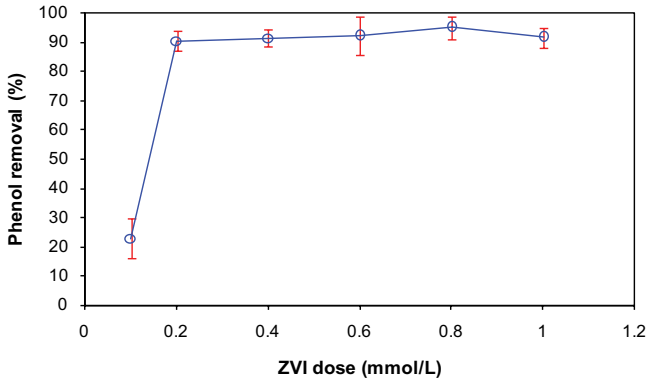

Fig. 5. Variation of phenol degradation efficiency under different ZVI dose (initial phenol concentration: 15 mg/L, solution pH: 5, PS dose: 0.2 mmol/L, and reaction time: 30 min).

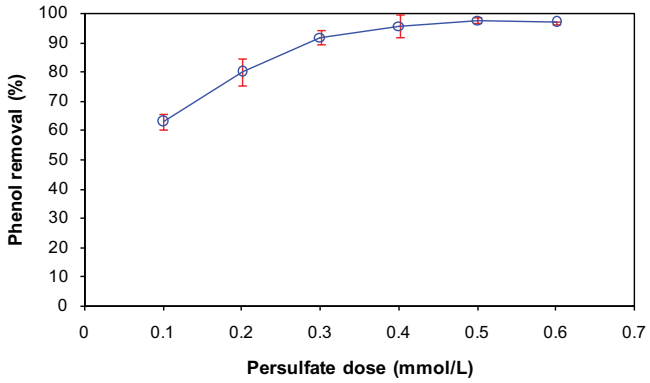

Fig. 6. Phenol degradation efficiency as a function of PS dose (initial phenol concentration: 15 mg/L, ZVI dose: 0.8 mmol/L, solution pH: 5, and reaction time: 30 min).

the $SO_4^{-\bullet}$ and $^{\bullet}OH$ radicals to less reactive $S_2O_8^{2-}$ radicals, reducing the process efficiency [41].

3.5. Effect of initial phenol concentration

The effect on the degradation rate of different initial phenol concentration was investigated in suspensions containing 0.8 mmol/L of ZVI, 0.5 mmol/L of PS radicals at an optimal solution pH of 5. The degradation rate of phenol measured under the initial concentration with increasing reaction time different is illustrated in Fig. 7.

As depicted in Fig. 7, a decrease in the phenol degradation efficiency was observed upon the increase of initial phenol concentration. With increasing initial phenol concentration from 5 to 35 mg/L, the phenol degradation efficiency reduced from 100% to 92.8%. In the ZVI/PS/UV process, the formation rate of reactive radicals would keep stable when the operational conditions are the same. Higher phenol concentration could consume more reactive radicals, that is, the concentration of reactive radicals in the solution would be decreased as a result of lowering the phenol degradation in the ZVI/PS/UV process. Nevertheless, the degradation rate of phenol gradually decreased as the increase of initial phenol concentration was also reported in some other AOPs [42].

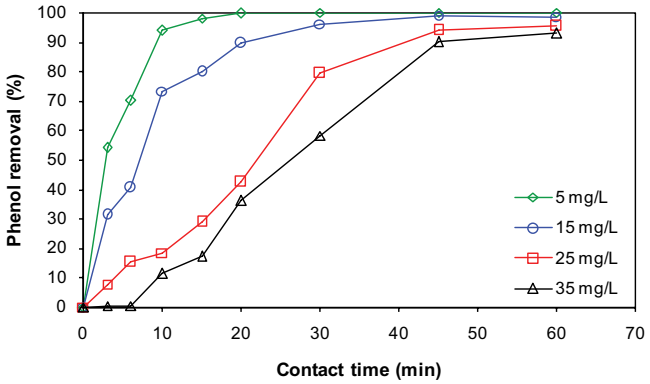

Fig. 7. Effect on initial phenol concentration on degradation efficiency (ZVI dose: 0.8 mmol/L, PS dose: 0.5 mmol/L, and solution pH: 5).

In addition, as observed in Fig. 7, the degradation efficiency of phenol increased fast at first 45 min, and then remained almost unchanged after 45 min. Thus, in the next experiments, the reaction time of 45 min was chosen.

3.6. Presence of co-existing cations and anions

Fig. 8 shows that all the five investigated co-existing cations including Na^+, K^+, Ca^{2+}, Mg^{2+}, and Al^{3+}, besides the seven chosen co-existing anions including F^-, Cl^-, HCO_3^-, NO_3^-, SO_4^{2-}, CO_3^{2-}, and PO_4^{3-} could affect the degradation efficiency of phenol in the combination of ZVI/PS/UV process.

As shown in Fig. 8, the presence of some co-existing anions showed inhibitory effects on phenol degradation efficiency including following a trend like $HCO_3^- > Cl^- > PO_4^{3-} > F^-$. As previously reported, HCO_3^- ions are common scavengers for reactive radicals [43]. In contrast, co-existing anions including NO_3^-, SO_4^{2-}, and CO_3^{2-} have shown the promoting effect on phenol degradation efficiency with an order of $CO_3^{2-} > NO_3^- > SO_4^{2-}$.

The enhanced phenol degradation by ZVI/PS/UV process is partially explained based on the formation of reactive radical species such as $SO_4^{-\bullet}$, $NO_3^{\bullet}$, and $CO_3^{-\bullet}$ from respective anions by interaction with $^{\bullet}OH$ in the bulk [44]. These species, though less reactive than $^{\bullet}OH$, are more abundant, not getting deactivated easily as in the case of $^{\bullet}OH$ radicals [45].

However, the phenol degradation efficiency by ZVI/PS/UV process with co-existing cations was repressed and varied in the following order:

$Al^{3+} > Ca^{2+} > Mg^{2+} > K^+ > Na^+$

On the one hand, trivalent cations were provided with high valency and total ion concentration compared to monovalent cations. The addition of cations led to the increased ionic strength, which hindered the electrostatic repulsive effects by a compression of the electric double layer. As cations with a strong electrostatic field (multi-charged) were the most efficient at compressing the electric double layer [46].

3.7. Effect of radical quenchers

The formation of activated radicals including $SO_4^{-\bullet}$ and $^{\bullet}OH$ as well as the oxidative intermediate species such as

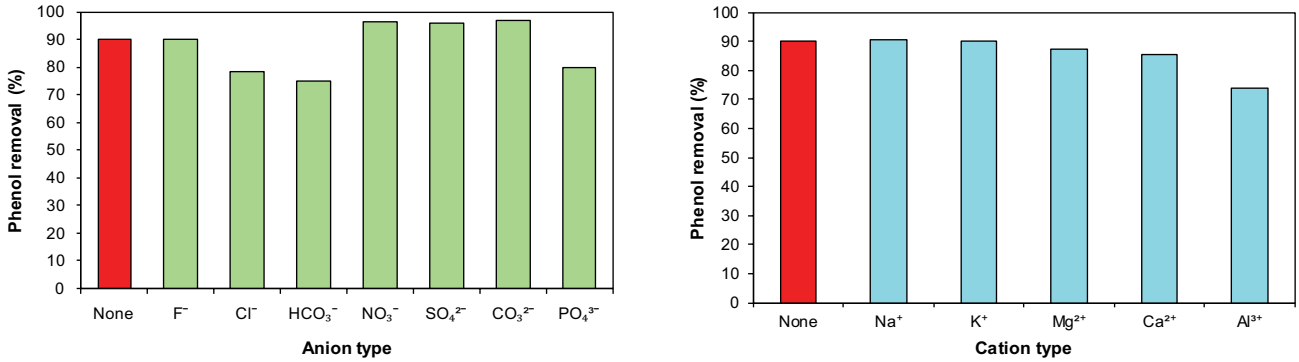

Fig. 8. Effect of co-existing anions on phenol degradation efficiency (initial phenol concentration: 35 mg/L, ZVI dose: 0.8 mmol/L, PS dose: 0.5 mmol/L, solution pH: 5, and reaction time: 45 min).

singlet oxygen ($^1O_2$) and superoxide ($O_2^{-\bullet}$) radicals under the combination of ZVI/PS/UV process has been indirectly investigated with the use of quenchers of these species. In these experiments, a comparison is made between the original phenol degradation efficiency values with those obtained after the addition of glucose as a quencher in the initial solution under otherwise identical conditions.

As shown in Fig. 9, the serious inhibition of phenol degradation efficiency is observed with increasing glucose concentration in the experiment. The control experiment showed the phenol removal efficiency of 89.97% and reduced to 66.98% at 25 mg/L of glucose concentration. When glucose was added, the $^{\bullet}OH$ and $SO_4^{-\bullet}$ radicals were consumed, leading to deterioration and degradation of phenol efficiency. Our results were similar to those acquired by the study by Liang and Su [47] who applied a chemical probe technology on thermally activated persulfate oxidation process to recognize the oxidizing species, and concluded that $OH^{\bullet}$ was the predominant radical at solution pH of 10.

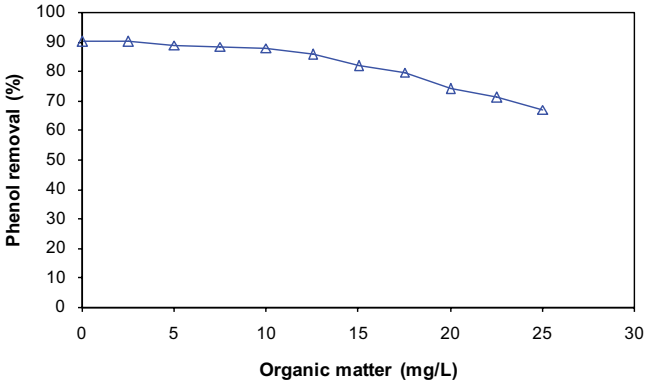

Fig. 9. Effect of organic matter on phenol degradation efficiency (initial phenol concentration: 35 mg/L, ZVI dose: 0.8 mmol/L, PS dose: 0.5 mmol/L, solution pH: 5, and reaction time: 45 min).

3.8. Phenol removal from real petrochemical wastewater

To examine the efficiency of the combination of ZVI/PS/UV process, real wastewater was collected from a petrochemical industry and subjected to phenol degradation with an optimized combination of ZVI/PS/UV process. The main characteristics of the petrochemical industry are summarized in Table 1.

Table 1
Characteristics of petrochemical industry

Parameter	Raw wastewater	After 2 h sedimentation
pH	7.1 ± 0.3	7.1 ± 0.2
tCOD concentration (mg/L)	220 ± 19	151 ± 11
sCOD concentration (mg/L)	132 ± 14	132 ± 9
Phenol concentration (mg/L)	3.46 ± 0.1	3.46 ± 0.1
TSS concentration (mg/L)	245 ± 26	90 ± 15

Due to high total suspended solids (TSS) in raw wastewater and lower UV penetration, the real wastewater was treated with simple sedimentation and then subjected to the combination of ZVI/PS/UV process treatment. Fig. 10 depicts the results of petrochemical industry wastewater with the combination of the ZVI/PS/UV process.

As illustrated in Fig. 10, for both experiments, nearly no phenol degradation efficiency was achieved after 45 min reaction time and the phenol degradation efficiency from raw and settled wastewater reached 73.12% and 42.77%, respectively.

3.9. ZVI reusability

The reusability of ZVI was assessed through five consecutive cycles of use under the optimal conditions (ZVI dose: 0.8 mmol/L, PS dose: 0.5 mmol/L, and solution pH: 5) for a 30 min period. The results regarding the phenol degradation efficiency for five cycles of ZVI/PS/UV are shown in Fig. 11. In each cycle of use, the catalyst was separated from the solution, washed several times with deionized water, and then applied for the next experiment without any modifications. After each recycling, the solution was analyzed to determine the phenol concentrations.

As depicted in Fig. 11, compared to 92.85% ± 0.51% of phenol degradation in the first cycle for ZVI, phenol removal efficiency reduced to 88.18% ± 3.91% by the fifth round. The catalytic performance of ZVI gradually

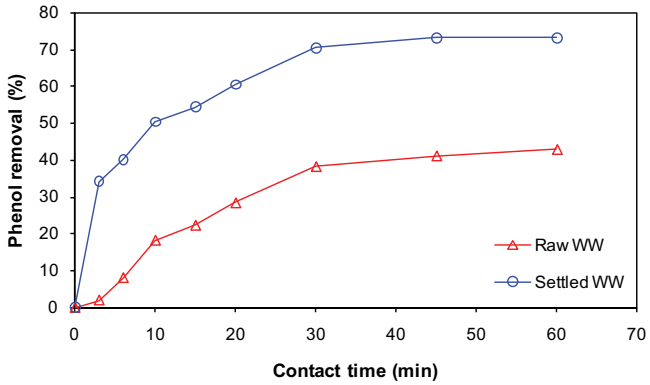

Fig. 10. Phenol degradation efficiency from real petrochemical wastewater (initial phenol concentration: 3.46 mg/L, ZVI dose: 0.8 mmol/L, PS dose: 0.5 mmol/L, and solution pH: 5).

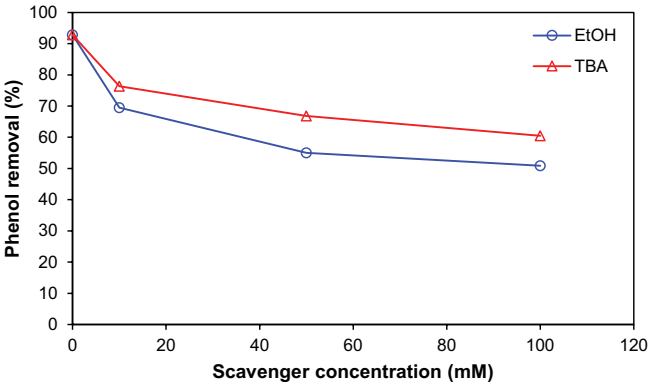

Fig. 12. Effect of scavengers on the phenol degradation (initial phenol concentration: 35 mg/L, ZVI dose: 0.8 mmol/L, PS dose: 0.5 mmol/L, solution pH: 5, and reaction time: 30 min).

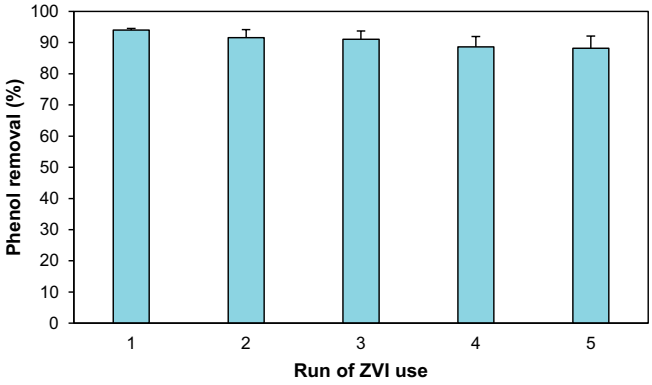

Fig. 11. Stability of ZVI in the multicycle phenol degradation (initial phenol concentration: 35 mg/L, ZVI dose: 0.8 mmol/L, PS dose: 0.5 mmol/L, solution pH: 5, and reaction time: 30 min).

weakened with repeated use, which could be related to the adsorption of intermediate products.

3.10. Possible mechanism

The $SO_4^{-\bullet}$ and $^{\bullet}OH$ are main radicals in AOP processes; and the *tert*-butyl alcohol (TBA) and ethanol (EtOH) were used as an effective scavenger of $^{\bullet}OH$, and both $^{\bullet}OH$ and $SO_4^{-\bullet}$, respectively [48]. As shown in Fig. 12, with EtOH and TBA addition, the phenol degradation efficiency by ZVI/PS/UV process markedly decreased.

The effects of EtOH and TBA on phenol degradation (Fig. 12) showed that EtOH had a much higher inhibitory effect on the phenol degradation compared to TBA. For instance, phenol degradation decreased by 50.91% in the presence of 100 mM EtOH when compared to the control experiment in which no scavenger was present, whereas inhibition of around 34.87% was observed in the presence of the same amount of TBA. This difference between the TBA and EtOH effects could be attributed to the contribution of $^{\bullet}OH$. Therefore, $SO_4^{-\bullet}$ was mainly responsible for phenol degradation during ZVI/PS/UV process. Fig. 12 indicates that the hydroxyl and sulfate radicals play an important role in phenol degradation. Therefore, a possible reaction mechanism in the degradation of phenol with the ZVI/PS/UV process is proposed in Fig. 13.

Firstly, persulfate can accelerate the corrosion rate of Fe^0. The Fe^0 corrosion process continuously releases large amounts of Fe^{2+}. Then, the Fe^{2+} produced facilitates PS activation to produce $SO_4^{-\bullet}$. The major reactions associated with ZVI activation of PS are expressed as Eqs. (9) and (10) [49]:

$$Fe^0 + S_2O_8^{2-} \rightarrow Fe^{2+} + 2SO_4^{2-} \quad (9)$$

$$Fe^{2+} + S_2O_8^{2-} \rightarrow Fe^{3+} + SO_4^{\bullet-} + SO_4^{2-} \quad (10)$$

In addition, H_2O_2 generated from Fe^0 oxidation by dissolved oxygen could react with Fe^{2+} to produce $^{\bullet}OH$ (Eqs. (11) and (12)) [50]:

$$Fe^0 + O_2 + 2H^+ \rightarrow Fe^{2+} + H_2O_2 \quad (11)$$

$$Fe^{2+} + H_2O_2 \rightarrow Fe^{3+} + {}^{\bullet}OH + OH^- \quad (12)$$

One of the advantages of this method is the Fe^{2+} regenerated by recycling Fe^{3+} at the surface of ZVI through Eq. (13) [51]:

$$Fe^0 + 2Fe^{3+} \rightarrow 3Fe^{2+} \quad (13)$$

In addition, iron hydroxides might generate during reaction through Eq. (14). They could remove phenol and its intermediates through adsorption:

$$Fe^{2+} + 2OH^- \rightarrow Fe(OH)^{2+} \quad (14)$$

The reasons for the positive effect of ultraviolet radiation on the reaction are explained in (Eqs. (15) and (16)) [52].

- The UV radiation in the system causes a Fenton-like reaction; so that ultraviolet radiation causes photolysis of iron hydroxides and as a result, the production of

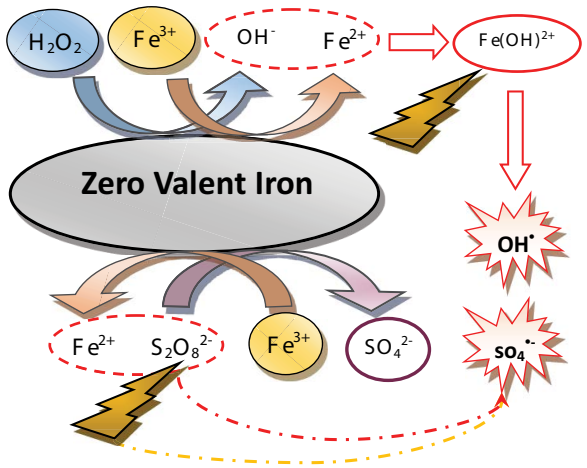

Fig. 13. Possible mechanism for phenol degradation in the ZVI/PS/UV process.

hydroxyl radicals, in turn accelerating the reaction.

$$Fe(OH)^{2+} \xrightarrow{h\nu} Fe^{2+} + {}^{\bullet}OH \quad (15)$$

- UV radiation can activate persulfate and produce sulfate radicals.

$$S_2O_8^{2-} \xrightarrow{h\nu} 2SO_4^{\bullet -} \quad (16)$$

- UV radiation also causes direct photolysis of phenol and thus increases its removal.

4. Conclusion

The degradation efficiency of a combination of ZVI and PS radical under UV irradiation for phenol degradation efficiency from synthetic wastewater were studied. Subsequently, a real petrochemical wastewater was treated with optimized combination of ZVI/PS/UV process. The main results of this study are as follows:

- The rate constant of a combination of ZVI/PS/UV process was fourfold that of the sum of the individual processes.
- With increasing solution pH from 2 to 5, the phenol degradation efficiency increased from 13.02% ± 1.67% to 86.89% ± 2.51%.
- With increasing ZVI does from 0.1 to 0.8 mmol/L, phenol degradation efficiency increased from 22.7% ± 6.93% to 94.87% ± 3.85%.
- Due to $SO_4^{\bullet -}$ consumption, application of PS dose higher than 0.5 mmol/L did not give rise to remarkable degradation performance.
- The HCO_3^- and Al^{3+} have shown the highest inhibitory effects on phenol degradation efficiency by ZVI/PS/UV process.
- The removal efficiencies of more than 73% were still obtained for phenol after five consecutive cycles of reaction.
- From the mechanism study, it was found out that phenol was degraded mainly through oxidation with $SO_4^{\bullet -}$ radicals.

Acknowledgments

The authors thank the Azad Islamic of Tabriz, Iran (grant no. 10250508972009) for the financial support of the present work.

References

[1] A. Ebrahimi, M.M. Amin, H. Pourzamani, Y. Hajizadeh, A.H. Mahvi, M. Mahdavi, M.H.R. Rad, Hybrid coagulation-UF processes for spent filter backwash water treatment: a comparison studies for PAFCl and $FeCl_3$ as a pre-treatment, Environ. Monit. Assess., 189 (2017) 1–15.
[2] M.M. Amin, B. Bina, E. Taheri, A. Fatehizadeh, M. Ghasemian, Stoichiometry evaluation of biohydrogen production from various carbohydrates, Environ. Sci. Pollut. Res., 23 (2016) 20915–20921.
[3] X. Liu, R. Ma, L. Zhuang, B. Hu, J. Chen, X. Liu, X. Wang, Recent developments of doped g-C_3N_4 photocatalysts for the degradation of organic pollutants, Crit. Rev. Environ. Sci. Technol., 10 (2020) 1–40.
[4] Y. Du, M. Zhou, L. Lei, Role of the intermediates in the degradation of phenolic compounds by Fenton-like process, J. Hazard. Mater., 136 (2006) 859–865.
[5] M. Zare, M.M. Amin, M. Nikaeen, B. Bina, H. Pourzamani, A. Fatehizadeh, E. Taheri, Resazurin reduction assay, a useful tool for assessment of heavy metal toxicity in acidic conditions, Environ. Monit. Assess., 187 (2015), doi: 10.1007/s10661-015-4392-y.
[6] W. Raza, J. Lee, N. Raza, Y. Luo, K.-H. Kim, J. Yang, Removal of phenolic compounds from industrial waste water based on membrane-based technologies, J. Ind. Eng. Chem., 71 (2019) 1–18.
[7] A. Akbari, M. Sadani, M.M. Amin, F. Teimouri, M. Khajeh, M. Mahdavi, M. Hadi, Managing sulfate ions produced by sulfate radical-advanced oxidation process using sulfate-reducing bacteria for the subsequent biological treatment, J. Environ. Chem. Eng., 6 (2018) 5929–5937.
[8] U. Maheswari.M, N.S. Ebenezer, J. Priyakumari.C, An *in silico* approach: homology modelling and docking studies of rabies virus glycoprotein with Salviifoside A of Alangium salviifolium, Int. J. Sci. Res., 78 (2015) 531–534.
[9] H. Farrokhzadeh, E. Taheri, A. Ebrahimi, A. Fatehizadeh, M.V. Dastjerdi, B. Bina, Effectiveness of *Moringa oleifera* powder in removal of heavy metals from aqueous solutions, Fresenius Environ. Bull., 22 (2013) 1516–1523.
[10] R. Sridar, U.U. Ramanane, M. Rajasimman, ZnO nanoparticles–synthesis, characterization and its application for phenol removal from synthetic and pharmaceutical industry wastewater, Environ. Nanotechnol. Monit. Manage., 10 (2018) 388–393.
[11] N.S. Alharbi, B. Hu, T. Hayat, S.O. Rabah, A. Alsaedi, L. Zhuang, X. Wang, Efficient elimination of environmental pollutants through sorption–reduction and photocatalytic degradation using nanomaterials, Front. Chem. Sci. Eng., 14 (2020) 1124–1135.
[12] J. Dosta, J. Nieto, J. Vila, M. Grifoll, J. Mata-Álvarez, Phenol removal from hypersaline wastewaters in a membrane biological reactor (MBR): operation and microbiological characterisation, Bioresour. Technol., 102 (2011) 4013–4020.
[13] E.B. Estrada-Arriaga, J.A. Zepeda-Aviles, L. García-Sánchez, Post-treatment of real oil refinery effluent with high concentrations of phenols using photo-ferrioxalate and Fenton's reactions with membrane process step, Chem. Eng. J., 285 (2016) 508–516.
[14] S. Mozia, Photocatalytic membrane reactors (PMRs) in water and wastewater treatment. A review, Sep. Purif. Technol., 73 (2010) 71–91.

[15] M. Sun, G. Feng, M. Zhang, C. Song, P. Tao, T. Wang, M. Shao, Enhanced removal ability of phenol from aqueous solution using coal-based carbon membrane coupled with electrochemical oxidation process, Colloids Surf., A, 540 (2018) 186–193.
[16] M. Mahdavi, A. Ebrahimi, A.H. Mahvi, A. Fatehizadeh, F. Karakani, H. Azarpira, Experimental data for aluminum removal from aqueous solution by raw and iron-modified granular activated carbon, Data Brief, 17 (2018) 731–738.
[17] S. Wang, A comparative study of Fenton and Fenton-like reaction kinetics in decolourisation of wastewater, Dyes Pigm., 76 (2008) 714–720.
[18] Y. Deng, R. Zhao, Advanced oxidation processes (AOPs) in wastewater treatment, Curr. Pollut. Rep., 1 (2015) 167–176.
[19] S.S. Sable, K.J. Shah, P.-C. Chiang, S.-L. Lo, Catalytic oxidative degradation of phenol using iron oxide promoted sulfonated-ZrO_2 by advanced oxidation processes (AOPs), J. Taiwan Inst. Chem. Eng., 91 (2018) 434–440.
[20] L. Mais, M. Mascia, S. Palmas, A. Vacca, Photoelectrochemical oxidation of phenol with nanostructured TiO_2-PANI electrodes under solar light irradiation, Sep. Purif. Technol., 208 (2019) 153–159.
[21] S. Garcia-Segura, E. Brillas, Applied photoelectrocatalysis on the degradation of organic pollutants in wastewaters, J. Photochem. Photobiol., C, 31 (2017) 1–35.
[22] P. Hu, M. Long, Cobalt-catalyzed sulfate radical-based advanced oxidation: a review on heterogeneous catalysts and applications, Appl. Catal., B, 181 (2016) 103–117.
[23] W. Chu, D. Li, N. Gao, M.R. Templeton, C. Tan, Y. Gao, The control of emerging haloacetamide DBP precursors with UV/persulfate treatment, Water Res., 72 (2015) 340–348.
[24] H. Lin, J. Wu, H. Zhang, Degradation of bisphenol A in aqueous solution by a novel electro/Fe^{3+}/peroxydisulfate process, Sep. Purif. Technol., 117 (2013) 18–23.
[25] Y.-C. Lee, S.-L. Lo, J. Kuo, C.-P. Huang, Promoted degradation of perfluorooctanic acid by persulfate when adding activated carbon, J. Hazard. Mater., 261 (2013) 463–469.
[26] Y. Ji, C. Dong, D. Kong, J. Lu, Q. Zhou, Heat-activated persulfate oxidation of atrazine: implications for remediation of groundwater contaminated by herbicides, Chem. Eng. J., 263 (2015) 45–54.
[27] X. Wang, L. Wang, J. Li, J. Qiu, C. Cai, H. Zhang, Degradation of Acid Orange 7 by persulfate activated with zero valent iron in the presence of ultrasonic irradiation, Sep. Purif. Technol., 122 (2014) 41–46.
[28] X. Zhou, Q. Wang, G. Jiang, P. Liu, Z. Yuan, A novel conditioning process for enhancing dewaterability of waste activated sludge by combination of zero-valent iron and persulfate, Bioresour. Technol., 185 (2015) 416–420.
[29] P. Neta, R.E. Huie, A.B. Ross, Rate constants for reactions of inorganic radicals in aqueous solution, J. Phys. Chem. Ref. Data, 17 (1988) 1027–1284.
[30] X. Guan, Y. Sun, H. Qin, J. Li, I.M. Lo, D. He, H. Dong, The limitations of applying zero-valent iron technology in contaminants sequestration and the corresponding countermeasures: the development in zero-valent iron technology in the last two decades (1994–2014), Water Res., 75 (2015) 224–248.
[31] X. Xie, Y. Zhang, W. Huang, S. Huang, Degradation kinetics and mechanism of aniline by heat-assisted persulfate oxidation, J. Environ. Sci., 24 (2012) 821–826.
[32] J. Du, W. Guo, H. Wang, R. Yin, H. Zheng, X. Feng, D. Che, N. Ren, Hydroxyl radical dominated degradation of aquatic sulfamethoxazole by Fe^0/bisulfite/O_2: kinetics, mechanisms, and pathways, Water Res., 138 (2018) 323–332.
[33] P. Xie, L. Zhang, J. Chen, J. Ding, Y. Wan, S. Wang, Z. Wang, A. Zhou, J. Ma, Enhanced degradation of organic contaminants by zero-valent iron/sulfite process under simulated sunlight irradiation, Water Res., 149 (2019) 169–178.
[34] E.W. Rice, R.B. Baird, A.D. Eaton, Standard Methods for the Examination of Water and Wastewater, 23rd ed., APHA, AWWA, WEF, 2017.
[35] L. Chen, X. Peng, J. Liu, J. Li, F. Wu, Decolorization of Orange II in aqueous solution by an Fe(II)/sulfite system: replacement of persulfate, Ind. Eng. Chem. Res., 51 (2012) 13632–13638.
[36] Y. Zhang, Q. Zhang, J. Hong, Sulfate radical degradation of acetaminophen by novel iron–copper bimetallic oxidation catalyzed by persulfate: mechanism and degradation pathways, Appl. Surf. Sci., 422 (2017) 443–451.
[37] P. Xie, Y. Guo, Y. Chen, Z. Wang, R. Shang, S. Wang, J. Ding, Y. Wan, W. Jiang, J. Ma, Application of a novel advanced oxidation process using sulfite and zero-valent iron in treatment of organic pollutants, Chem. Eng. J., 314 (2017) 240–248.
[38] Y. Du, M. Dai, J. Cao, C. Peng, I. Ali, I. Naz, J. Li, Efficient removal of acid orange 7 using a porous adsorbent-supported zero-valent iron as a synergistic catalyst in advanced oxidation process, Chemosphere, 244 (2020)125522.
[39] S.-Y. Oh, S.-G. Kang, P.C. Chiu, Degradation of 2,4-dinitrotoluene by persulfate activated with zero-valent iron, Sci. Total Environ., 408 (2010) 3464–3468.
[40] T.S. Rad, A. Khataee, S. Rahim Pouran, Synergistic enhancement in photocatalytic performance of Ce(IV) and Cr(III) co-substituted magnetite nanoparticles loaded on reduced graphene oxide sheets, J. Colloid Interface Sci., 528 (2018) 248–262.
[41] A. Khataee, T.S. Rad, B. Vahid, S. Khorram, Preparation of zeolite nanorods by corona discharge plasma for degradation of phenazopyridine by heterogeneous sono-Fenton-like process, Ultrason. Sonochem., 33 (2016) 37–46.
[42] R.J. Wood, C. Vévert, J. Lee, M.J. Bussemaker, Flow effects on phenol degradation and sonoluminescence at different ultrasonic frequencies, Ultrason. Sonochem., 63 (2020)104892.
[43] P. Xie, J. Ma, W. Liu, J. Zou, S. Yue, X. Li, M.R. Wiesner, J. Fang, Removal of 2-MIB and geosmin using UV/persulfate: contributions of hydroxyl and sulfate radicals, Water Res., 69 (2015) 223–233.
[44] C. Minero, P. Pellizzari, V. Maurino, E. Pelizzetti, D. Vione, Enhancement of dye sonochemical degradation by some inorganic anions present in natural waters, Appl. Catal., B, 77 (2008) 308–316.
[45] K.P. Jyothi, S. Yesodharan, E.P. Yesodharan, Influence of commonly occurring cations on the sono, photo and sonophoto catalytic decontamination of water, IOSR J. Appl. Chem., 2016 (2016) 15–24.
[46] Y. Jiang, Y. Luo, Z. Lu, P. Huo, W. Xing, M. He, J. Li, Y. Yan, Influence of inorganic ions and pH on the photodegradation of 1-methylimidazole-2-thiol with TiO_2 photocatalyst based on magnetic multi-walled carbon nanotubes, Bull. Korean Chem. Soc., 35 (2014) 76–82.
[47] C. Liang, H.-W. Su, Identification of sulfate and hydroxyl radicals in thermally activated persulfate, Ind. Eng. Chem. Res., 48 (2009) 5558–5562.
[48] S. Hadi, E. Taheri, M.M. Amin, A. Fatehizadeh, T.M. Aminabhavi, Synergistic degradation of 4-chlorophenol by persulfate and oxalic acid mixture with heterogeneous Fenton like system for wastewater treatment: adaptive neuro-fuzzy inference systems modeling, J. Environ. Manage., 268 (2020) 110678
[49] X. Zou, T. Zhou, J. Mao, X. Wu, Synergistic degradation of antibiotic sulfadiazine in a heterogeneous ultrasound-enhanced Fe^0/persulfate Fenton-like system, Chem. Eng. J., 257 (2014) 36–44.
[50] Q. Wang, S. Tian, P. Ning, Degradation mechanism of methylene blue in a heterogeneous Fenton-like reaction catalyzed by ferrocene, Ind. Eng. Chem. Res., 53 (2014) 643–649.
[51] P. Jia, H. Tan, K. Liu, W. Gao, Synthesis, characterization and photocatalytic property of novel ZnO/bone char composite, Mater. Res. Bull., 102 (2018) 45–50.
[52] P.K. Labhane, G.H. Sonawane, S.H. Sonawane, Influence of rare-earth metal on the zinc oxide nanostructures: application in the photocatalytic degradation of methylene blue and p-nitro phenol, Green Process. Synth., 7 (2018) 360–371.